Original Article

Design of Model Following Control Integrating PID Controller for DC Servomotor-Based Antenna Positioning System

Isdore Onyema Akwukwaegbu[1], Nosiri Onyebuchi Chikezie[2], Mathew Olubiwe[3],
Paulinus-Nwammuo Chiedozie Francis[4], Emmanuel Okoronkwo[5]

[1,2,3,4,5]*Department of Electrical and Electronic Engineering, The Federal University of Technology, Owerri, Nigeria.*

[2]*Corresponding Author : onyebuchi.nosiri@futo.edu.ng*

Abstract - *The study presented the design of an efficient motorized antenna positioning control system using Model Following Control (MFC). It was desired to design a control system to improve system stability and reduce position error. The dynamic model of a direct current (DC) servomotor antenna control system was developed to achieve this. An MFC was designed that integrated a Proportional Integral Derivative (PID) controller in the frequency domain for tuning the control loop in terms of transient characteristics and robustness; this gives a technique known as MFC-PID control. The MFC-PID was integrated with the dynamic model of the DC servo motor antenna closed-loop control system. The designed system was simulated in MATLAB/SIMULINK environment. The system was able to achieve the performance criteria in terms of rise time ($t_r = 1.4483s$), settling time ($t_s = 4.2470s$) and overshoot ($M_p = 5.5214\%$), which represents an improvement on the settling time and overshoot over the convectional PID technique. Generally, the performance of the antenna positioning servo control system was optimized using the MFC-PID algorithm.*

Keywords - Antenna, Model following control, MFC-PID controller, Position control, DC servomotor.

1. Introduction

Direct Current (DC) servomotor designed for parabolic antenna positioning and speed tracking system has attracted much study in control systems. The antenna pointing angle of the ground station must be aligned carefully to ensure it is pointing accurately in the direction of the target satellite [1]. Communication over the wireless network requires the parabolic dish of a ground station antenna to be properly positioned for effective azimuth/elevation placement. This ensures reliable and stable satellite communication. One approach to achieving this is a DC servomotor-based antenna positioning control system.

The most common problem with antenna employed in satellite communication is positioning, which requires aligning the dish to aim at the correct satellite location for proper communication [2]. Since every antenna is dedicated to a specific satellite, it is not easy to point it at the appropriate satellite [3]. Therefore, an automated system must be integrated with the system to realize the optimum positioning for quality signal transmission and reception.

It is possible to achieve cost-effectiveness concerning the anticipated link margin necessary to receive most satellite transmission data from a certain angle of elevation (or azimuth position). In order to achieve this, a compensator (Controller) is added as a subsystem and connected to the existing antenna system to improve its performance. A compensator provides the required command to the system to achieve the desired performance response.

This way, the control system ensures stability, a steady state, improved transient responses, cost, and robustness. These requirements apply to the satellite ground station's antenna servo control system design. The objective is to have a system with robust tracking, reduced steady-state error, and improved transient response.

The angular positioning (azimuth/elevation) performance of parabolic antenna suffers from environmental disturbance problems such as wind, which adversely affects reception, resulting in reduced signal quality or, in some cases, total signal loss. Over the years, many control measures have been employed to overcome this problem.

The transient and steady performance of satellite dish antenna mounted on distributed mobile telemedicine nodes (DMTNs) was improved using a complete satellite feedback

controller [4]. Proportional-Integral-Derivative (PID) tuned compensator (PID-TC) was used to enhance the error observed in tracking and robustness of the servo positioning control system of the DC servo-based parabolic antenna [5, 6]. Also, the cost-effective performance of ground station satellite antenna, PID tuned digital compensator (PID-TDC) was implemented in [7].

The effects of complete state feedback control, PID control, and proportional plus prefilter control schemes on dish antenna positioning system for telemedicine was evaluated by [8]. A control system based on PID and discrete PID was used to enhance the position control of a Giant Meter Wave Radio Telescope (GMRT) [9]. A hybrid PID-Linear Quadratic Regulator (LQR) was implemented for DC servomotor-based antenna positioning system [10]. PID and LQR controllers were applied in the radio telescope antenna azimuth position control system [11]. State feedback and PID controllers were used to improve the overall control of an antenna azimuth position [12].

In order to address the position control of antenna azimuth, the authors of [13] proposed a fractional order lead compensator including Ziegler Nichols tuned proportional Integral (PI) Controller and conventional lead compensator based on desired phase margin. In [14], the minimum deviation angle after rotation of the antenna was aimed using the PID controller, Fuzzy Logic Controller (FLC) and Sliding Mode Controller (SMC). The performance response of the mobile satellite dish antenna network was enhanced by [15]. Improved antenna azimuth position control system stability was achieved using Model Reference Adaptive Control (MRAC) based on Lyapunov and gradient approach.

Similarly, MRAC and self-tuning controller (STC) was implemented to adaptively respond to changes in environmental conditions and minimise the antenna deviation concerning its reference position [16]. An optimal PID controller tuning for deep space antenna azimuth position has been achieved using a weighted cultural artificial fish swarm algorithm (wCAFSA) [17]. The problem of antenna alignment in dynamic point-to-point communication for the high-quality transmit-receive signal operation was solved using the Least Square Method (LSM) [18] to tune the optimal level signal value (LSV) point, which was dependent on the Coordinate Coarse Tracking Alignment (CCTA) and Matrix Scanning Strategy (MSS) to determine the LSV.

With significant studies on antenna positioning control, each control strategy has limitations. Conventional controllers such as PID, lead compensator, and state feedback controller suffer changes in system parameters and nonlinear effects [19]. The drawback of only FLC is that it leads to steady-state error [20, 21]. As for SMC, it is prone to chattering. As the system approaches the setpoint, the performance of PID-LQR degrades due to nonlinearity and delay.

This study aims to reduce the positioning error of a DC servomotor-based antenna using Model Following Control (MFC) plus PID controller (MFC-PID). In a situation such as the case of a servo motor system that is prone to internal nonlinearity like friction and external perturbation like wind force which causes error in realizing the desired response position and speed of the motor, the PID alone may not be effective. The practical design combination of the MFC and PID control method implemented in the study provides many benefits compared with the existing systems. Some characteristics are summarized as follows: (i) it produces a control or manipulated signal before the occurrence of the error, and (b) it uses well-designed reference signals to make the process track the reference without saturating the control signal.

2. Method

The design strategy starts with problem formulation and modeling of the system. This is followed by control algorithm development, which includes: Proportional Integral and Derivative (PID) controller and Model Following Controller (MFC). The designed control algorithms are integrated with the system model of a parabolic antenna positioning based on DC servomotor. The developed control loop is implemented in MATLAB/Simulink environment.

The MATLAB codes and the Simulink embedded blocks are the primary tools or materials used for the modeling and simulations. Another tool used is the PID tuner, a MATLAB application. The MATLAB codes were used to analyse the open and closed loop transfer functions, including system performance characteristics.

2.1. DC Motor and Load

The mathematical equations describing the servo mechanism of a DC motor-based antenna positioning system for satellite tracking (controlling azimuth or elevation) are presented in this subsection. The variable representing the DC servomotor, inputs, outputs signals and their corresponding parameter values are defined and tabulated in Table 1.

A schematic illustration of armature controlled DC motor is shown in Figure 1 and comprises the armature resistance, R_a armature inductance, L_a, the voltage across the armature, V_a, the back emf, the motor shaft, motor inertia, load inertia, J_m, B_a and the angular position of the shaft $\theta(t)$.

The armature-voltage relationship equations are obtained by using the electrical circuit law called Kirchhoff's voltage law (KVL) and the dynamic equation law of Newton for the DC motor operation as shown in [5, 22]:

$$V_a(t) = R_a I_a(t) + L_a \frac{dI_a(t)}{dt} + E_b(t) \tag{1}$$

$$E_b(t) = K_B \omega_m(t) = K_B \frac{d\theta(t)}{dt} \qquad (2)$$

$$T_m(t) = K_T I_a(t) \qquad (3)$$

Where $E_b(t)$ is back electromotive force (e.m.f), $T_m(t)$ is motor torque, K_B is back e.m.f constant, $\omega_m(t)$ is the angular speed velocity, and K_T is motor torque constant. Expressing Eq. (1) in terms of Eq. (2) gives [5, 23, 24]:

$$V_a(t) = L_a \frac{dI_a(t)}{dt} + R_{a}I_a(t) + K_B \frac{d\theta(t)}{dt} \qquad (4)$$

The torque equation can further be expressed by:

$$J_a \frac{d^2\theta(t)}{dt} + B_a \frac{d\theta(t)}{dt} = K_T I_a(t) \qquad (5)$$

The Laplace transforms of Eq. (4) and (5) taking zero initial conditions is defined by [5, 23]:

$$V_a(s) = L_a s I_a(s) + R_a I_a(s) + K_B s\theta(s) \qquad (6)$$

$$J_a s^2 \theta(s) + B_a \theta(s) = K_T I_a(s) \qquad (7)$$

Equating Eq. (6) and (7) in terms of current gives:

$$\frac{V_a(s) - K_B s\theta(s)}{R_a + L_a s} = \frac{J_a s^2 \theta(s) + B_a s\theta(s)}{K_T} \qquad (8)$$

The ratio of the angular position (output), $\theta(s)$ and the applied voltage (input), $V_a(s)$ is defined by [5, 23]:

$$\frac{\theta(s)}{V_a(s)} = \frac{K_T}{s[(R_a + L_a s)(J_a s + B_a) + K_T K_B]} \qquad (9)$$

The block diagram representing the closed-loop control system of the DC motor is shown in Figure 2.

Assuming zero disturbance, the ratio of the reference input voltage to the angular velocity called the system transfer function, as shown in Figure 2, is given by [5, 23]:

$$\frac{\omega(s)}{V_a(s)} = \frac{K_T}{[(R_a + L_a s)(J_a s + B_a) + K_T K_B]} \qquad (10)$$

Table 1. Parameters of DC servomotor model [5, 10, 22, 23]

| Definition of Quantity	Numerical Value
Power Amplifier Pole	100
Motor and Load Pole	1.71
Motor Dampening Constant [Nm/rad]	0.01
Load Dampening Constant [Nms/rad]	1
Equivalent Viscous Friction Coefficient [Nms/rad]	0.02
Motor Inertia constant [kgm^2]	0.02
Load Inertia constant [kgm^2]	1
Equivalent moment of Inertia [kgm^2]	0.03
Preamplifier Gain	-
Power Amplifier Gain	100
Back emf Constant [Vs/rad]	0.5
Gear Ratio	0.1
Motor and Load Gain	2.083
Potentiometer Gain	0.318
Motor Torque Constant [Nm/A]	0.5
Motor Armature Inductance [H]	0.45
Turns on Potentiometer	10
Gear Teeth (Respectively)	25, 250, 250
Motor Armature resistance [Ω]	8
Voltage Across Potentiometer [V]	10
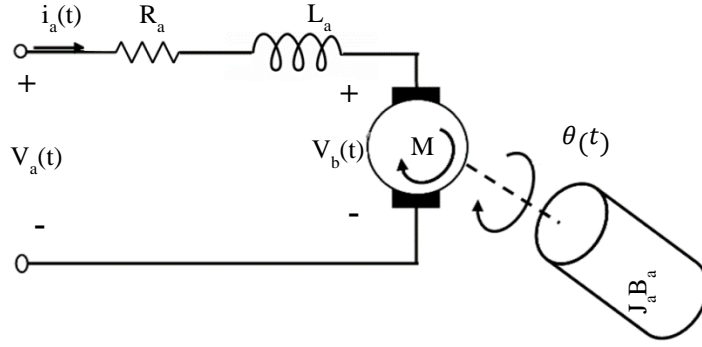
Fig. 1 DC motor circuit diagram [5]
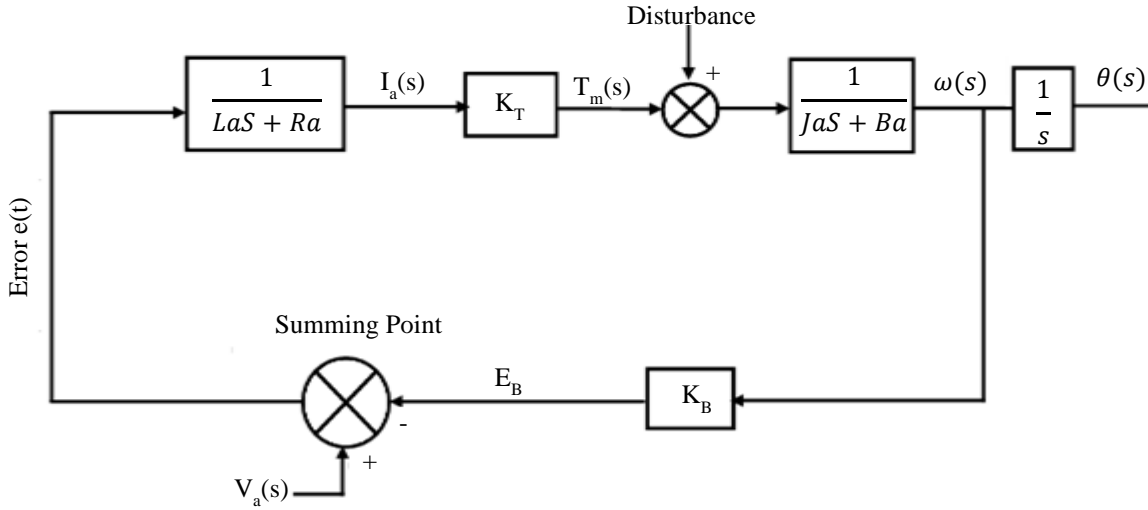
Fig. 2 Closed loop block diagram of DC servomotor [5, 23]

The inductance, L_a, of the armature circuit is often negligible for a fixed motor and $K_T = K_a R_a >> L_a$ [5,10,23]. Therefore Eq. (10) simplifies to:

$$\frac{\theta(s)}{V_a(s)} = \frac{K_T/R_a}{J_a s^2 + s\left(B_a + K_T K_B/R_a\right)} \tag{11}$$

Substituting the equivalent values for the moment of inertia and the viscous friction coefficient into Eq. (11) results in [5,23]:

$$\frac{\theta(s)}{V_a(s)} = \frac{K_T/R_a J_m}{J_m s^2 + s\left(B_m + K_T K_B/R_a\right)} \tag{12}$$

The numerator and the denominator of Eq. (12) are divided by J_m to give the expression:

$$\frac{\theta(s)}{V_a(s)} = \frac{K_m}{s(s+a_m)} \tag{13}$$

With: $K_m = \dfrac{K_T}{R_a J_m}$ and $a_m = \dfrac{B_m R_a + K_T K_B}{J_m R_a}$, such that K_m stands for the motor and load gain, and a_m is the motor and load pole.

Figure 3 is a closed-loop diagram of the system, which shows that the loop comprises a preamplifier, a power amplifier, a motor and a load. Considering the gear ratio (K_g), and the transfer function for the angular position and the armature voltage gives [5, 23]:

$$\frac{\theta(s)}{V_a(s)} = 0.1 \times \frac{K_m}{s(s+a_m)} = \frac{0.2083}{s(s+1.71)} \tag{14}$$

Substituting the values of the parameters given in Table 1 for the closed-loop control of antenna positioning without Controller in Figure 3 gives the transfer function from the input position to the output position defined by:

$$\frac{\theta_o(s)}{\theta_i(s)} = \frac{6.63K}{s^3 + 101.71s^2 + 171s + 6.63K} \tag{15}$$
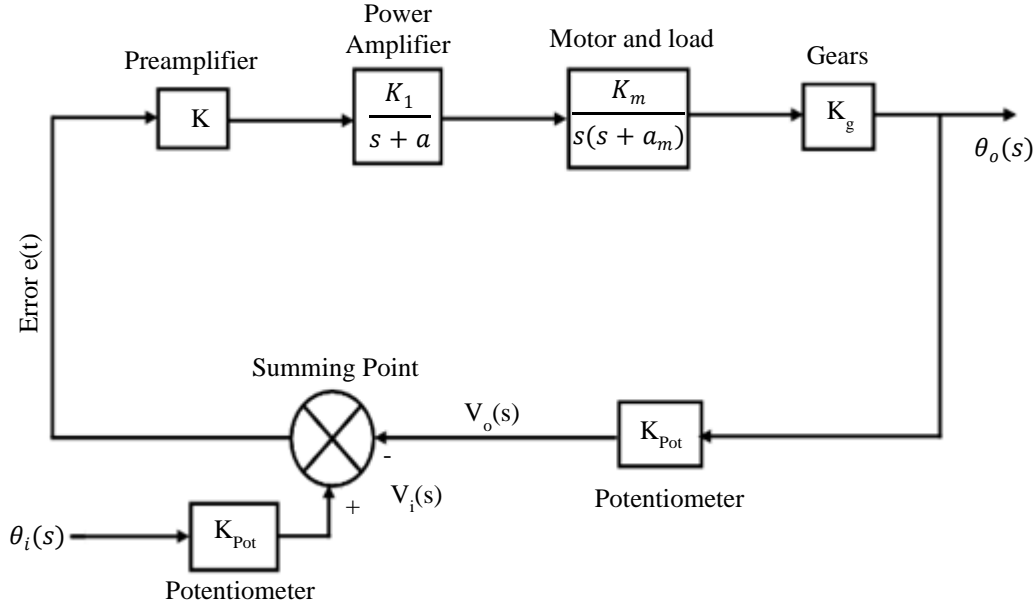
Fig. 3 The block diagram of the close-loop antenna DC servomotor control system (without a controller)

The closed loop poles are expected to be on the left half of the complex frequency plot (s-plane) to achieve a stable system. Changing the loop gain also brings about a change in the locations of the poles. This allows the poles to move into the right half side of the s-plane, thereby leading to instability. As a result, it is proper to have a gain setting to ensure the stability of a closed-loop control system during formulation. The preamplifier gain K required to maintain the stability of the closed-loop control system is determined in this work using the Routh-Hurwitz criterion.

This value of K will make the system to be marginally stable. Hence, it produces no changes in the sign in column one if $0 < K < 2623.29$, which serves as the stability condition [6]. This paper chooses the gain K as 100 obtained using the Routh Hurwitz criterion [5, 11, 26].

$$G_p(s) = \frac{\theta_o(s)}{\theta_i(s)} = \frac{663}{s^3+101.71s^2+171s+663} \quad (16)$$

2.2. Design of PID Controller
The PID controller is viewed as an acceptable controller deployed in industrial control systems for a three-term control-loop feedback system [23]. The Controller leverages a command signal to regulate and minimize the system error[27]. It also provides optimal control dynamics, including zero steady-state error, fast response (short rise time), minimized overshoot, no oscillations and higher stability [28]. The main advantage the application of PID controller has when compared with some linear controllers is its potential use in higher-order processes over other linear controllers [29]. A block diagram of a PID control system is shown in Figure 4.
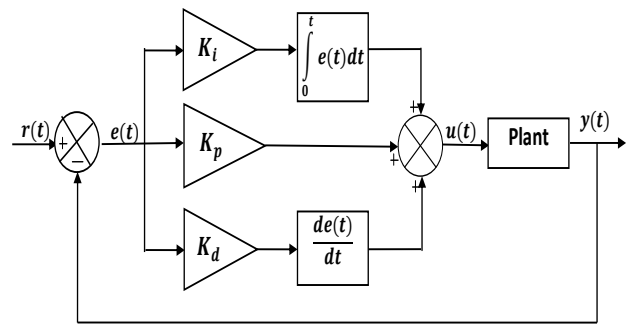

Fig. 4 Model of PID control system [26]

The mathematical description of the PID control algorithm can be determined in Figure 4. The quantities $r(t)$, $e(t)$, $u(t)$ are considered as the reference input (position), error (or deviation of the actual antenna position from the reference position), and controller output. The PID controller parameters (K_p, K_i, K_d) are referred to as the proportional, integral and derivative gains respectively, and $y(t)$ as the output (in this case, the actual antenna position).

$$e(t) = r(t) - y(t) \quad (17)$$

PID computations are performed based on the error obtained from the summing point when fed into the PID controller. Hence, the controller output is given by [21]:

$$u(t) = K_p e(t) + K_i \int_0^t e(t)\mathrm{dt} + K_d \frac{\mathrm{de}(t)}{\mathrm{dt}} \quad (18)$$

Equation (18) shows the continuous time ideal PID controller in the time domain and could be represented in Laplace transform assuming zero initial condition as [21]:

$$U(s) = K_p E(s) + K_i \frac{1}{s} E(s) + K_d s E(s) \qquad (19)$$

Or in a simplified form as

$$C(s) = K_p + K_i \frac{1}{s} + K_d s \qquad (20)$$

Where $C(s) = U(s)/E(s)$ and is called the PID controller.

The actual PID controller, which most often is realized in practice by using prefilter i, with its derivative components to tackle the issues of noise that may go into the Controller via the derivative part, is given by [23]:

$$C(s) = K_p + K_i \frac{1}{s} + K_d \left(\frac{sN}{s+N} \right) \qquad (21)$$

There are various ways of tuning the PID to achieve a desired goal. However, in this study, the PID was tuned directly using the MATLAB tool and its equation is obtained as follows:

$$C(s) = 21.0191 + 7.942 \frac{1}{s} + 9.5057 * \frac{100s}{s+100} \qquad (22)$$

Where the coefficient of the low pass filter, N, is 100.

2.3. Design of Model Following Controller

In particular design cases, when ensuring more accurate control of the output response is desirable, a reference model that provides the desired output to the setpoint (input) changes is implemented. An easy method is to use the structure shown in Figure 5 such that the output of the reference model is fed into a feedback control loop.

The reference model is usually a first- or second-order dynamic system. A model following Controller is achieved by joining a simple controller in a feedback loop with a model.

However, the system presented in Figure 5 can be improved considerably by adding a feed-forward in the control loop, as shown in Figure 6. The signal u_{ff} is such that it will yield the desired controlled signal (output response), provided the models are accurate. The error e will differ from zero when the output changes from its desired characteristics. The feedback path will then generate the appropriate actions.

In the model following control, the reference model (or trajectory planner) $G_m(s)$ and the model following controller, $G_m(s)/G_p(s)$, are designed such that the feed-forward input signal u_{ff} drives the output to the desired setpoint, R_{sp}. The design can be achieved in either the time or frequency domains (as a transfer function).
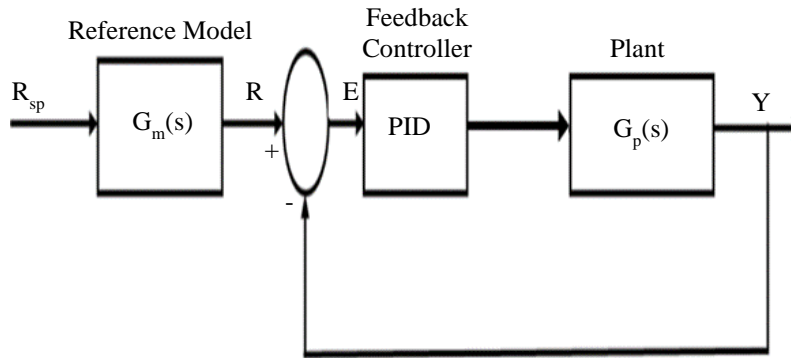

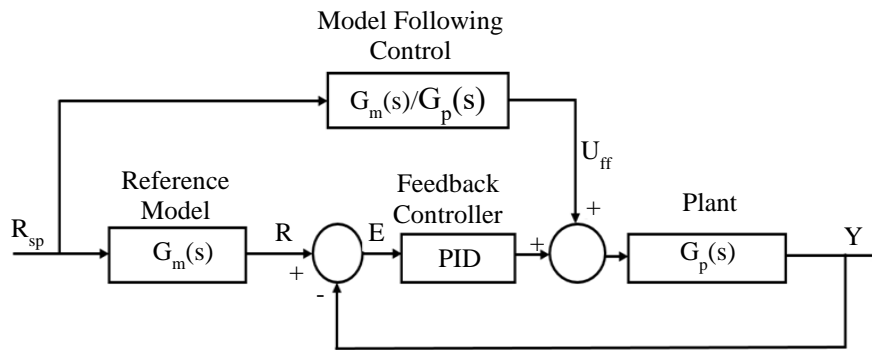**Fig. 5 Feedback control loop with the reference model**

Fig. 6 Model following controller structure

There is a need to generate $G_m(s)$. In order to realize this, a second-order transfer function is chosen because the servo system under consideration has a second-order dynamic equation for the speed given by Equation (23). This is used to establish the characteristics and performance of the positioning system approximately. Therefore, the characteristics equation of a second-order system is defined by:

$$G_m(s) = \frac{\omega_n^2}{s^2 + 2\zeta\omega_n s + \omega_n^2} \qquad (23)$$

Where ω_n is the natural frequency response, and ξ is the damping ratio of the system. These parameters are determined as follows:

$$M_p = e^{-\pi\xi/\sqrt{1-\xi^2}} \qquad (24)$$

Where M_p is the peak value equal to 10% (or 0.1), ξ is the damping ratio, and $\pi = 22/7$ or 3.142. Substituting these values into Equation (24) gives:

$$\log_e 0.1 = \log_e e^{-3.142\xi/\sqrt{1-\xi^2}} \qquad (25)$$

Solving Equation (25), the value of the damping ratio, $\xi = 0.6$.

The relationship between the settling time t_s, the damping ratio ξ and the natural frequency response ω_n, is given by:

$$t_s = \frac{4}{\xi\omega_n} \qquad (26)$$

Substituting 5s for t_s and 0.6 for ξ into Equation (26) gives $\omega_n = 1.33$ rad/s. substituting these values into Equation (23) gives:

$$G_m(s) = \frac{1.7689}{s^2 + 1.596s + 1.7689} \qquad (27)$$

With the servo positioning system in Equation (16) represented as $G_p(s)$, the model following control or feed-forward Controller is given by:
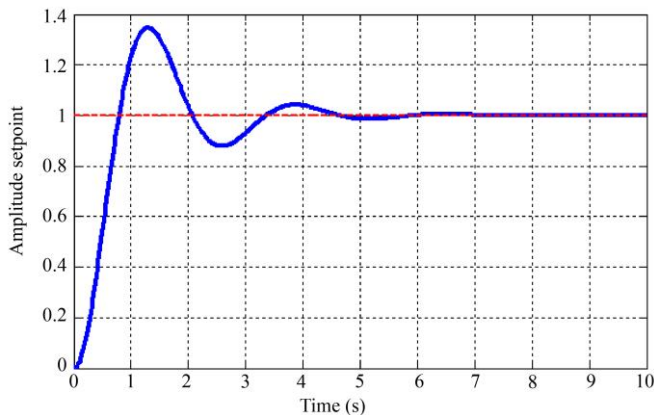

Fig. 7 Open loop step response (uncompensated)

$$\frac{G_m(s)}{G_p(s)} = 0.0027 \times \frac{s^3 + 101.71s^2 + 171s + 663}{s^2 + 1.596s + 1.7689} \qquad (28)$$

3. Results and Discussion

The proposed Model Following Controller and Proportional Integral Derivative (MFC-PID) control technique for the antenna positioning servo control system has been addressed by MATLAB/Simulink environment simulation. In addition, the MFC-PID controller has been compared with the PID controller to perform performance evaluation. Simulation has been carried out considering uncompensated scenario (or open loop) and compensated scenario (closed loop) antenna positioning servomotor.

The simulation was based on the step response of the uncompensated antenna positioning servo control system shown in Figure 7. Figure 8 presents the step response of the antenna positioning servo control system compensated with a PID controller. The step response of an antenna positioning servo control system compensated with an MFC-PID controller is shown in Figure 9. The step response comparison of the PID controller and MFC-PID Controller is shown in Figure 10. Step response performance characteristics evaluation of the simulation results has been presented in Table 2.
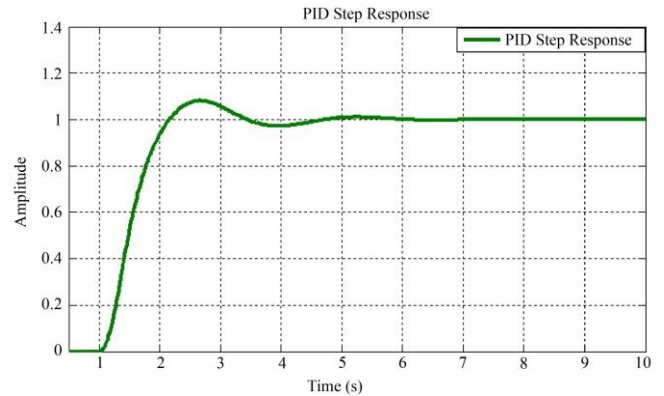

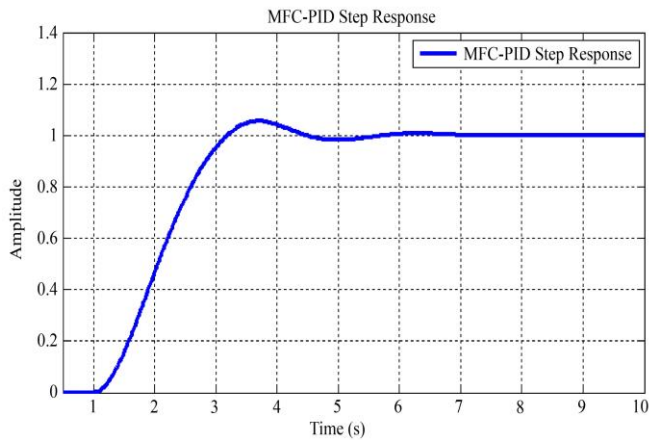**Fig. 8 PID compensated closed-loop step response**

Fig. 9 MFC-PID compensated closed-loop step response

Table 2. Step response performance characteristics

System	t_r (s)	t_s (s)	M_p (%)	e_{ss}	Remark
Open loop	0.52	5.34	34.6	0	Unsatisfactory
PID	0.73	4.28	8.09	0	satisfactory
MFC-PID	1.44	4.24	5.52	0	Satisfactory

Note: t_r is rise time, t_s settling time, M_p is peak overshoot, and e_{ss} is a steady-state error.
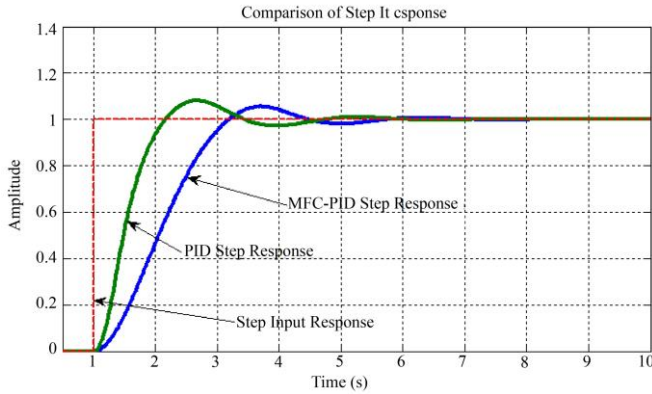

Fig. 10 PID and MFC-PID step response comparison

The response performance characteristics regarding rise time, settling time, percentage overshoot, and steady-state error have been evaluated. Figure 7 presents the step response of the antenna positioning servo control system model without a controller. The simulation result shows that the system has a high degree of instability with an overshoot value of 34.6%. This is unsatisfactory and, as such requires improvement.

The step response plot of the antenna positioning servo control system with a tuned PID controller presented in Figure 8 indicates an improved performance characteristic that meets the design specifications with a reduced overshoot value of 8.0963% and a steady-state error value of 0.

Figure 9 is the simulation plot for the unit step response of the antenna positioning servo control system model with an MFC-PID controller. The performance response evaluation in

Table 2 indicates that the MFC-PID control technique reduced the overshoot value to 5.52% with a steady state error value of 0.

Generally, the step response performances show that the implemented MFC-PID control technique met the design criteria with improved stability.

4. Conclusion

A Model Following Controller (MFC) design that combines Proportional Integral and Derivative (PID) algorithm to give an MFC-PID Controller for D.C. servomotor-based antenna positioning system has been effectively achieved. This was established through simulation conducted in MATLAB/Simulink environment for Simulated output responses of antenna positioning servo control system to step input signal, which met the design specifications. Also, the simulation results obtained showed that the MFC-PID control technique could be set up to drive the azimuth/elevation Direct Current (DC) servomotors to direct a parabolic dish antenna and ensures that it is always kept within the referenced line of sight with a particular satellite. Generally, the performance of the antenna positioning servo control system was optimized to establish a more robust and improved tracking response of the satellite communication system using the MFC-PID algorithm.

References

[1] Wei Fan et al., "In Situ Antenna Pointing Angle Calibration for Q-Band Satellite Ground Station," *IEEE Antenna and Wireless Propagation Letters*, vol. 19, no. 7, pp. 1246-1250, 2020. [CrossRef] [Google Scholar] [Publisher Link]

[2] Hassan, Ahmad Kama, and Hoque, Ahsanul, "*Automated Microwave Antenna Alignment of Base Transceiver Station*," A Thesis Submitted to the Faculty of Karlstad University, Faculty of Technology and Science Department of Physics and Electrical Engineering, pp. 1-33, 2011. [Publisher Link]

[3] Prasanna Sugandhi et al., "Automatic Antenna Positioning System," *International Journal for Scientific Research and Development,* vol. 4, no. 3, pp. 372 –374, 2016. [Publisher Link]

[4] Bonaventure Onyeka Ekengwu et al., "Satellite Dish Antenna Control for Distributed Mobile Telemedicine Nodes," *International Journal of Informatics and Communication Technology,* vol. 11, no. 3, pp. 206–217, 2022. [CrossRef] [Google Scholar] [Publisher Link]

[5] Paulinus Chinaenye Eze, Chidiebere Alison Ugoh, and D. S. Inaibo, "Positioning Control of DC Servomotor-Based Antenna using PID Tuned Compensator," *Journal of Engineering Sciences*, vol. 8, no. 1, pp. 9-16, 2021. [CrossRef] [Google Scholar] [Publisher Link]

[6]   Paulinus Chinaenye Eze et al., "Improving the Performance Response of Mobile Satellite Dish Antenna Network within Nigeria," *Journal of Electrical Engineering, Electronics, Control and Computer Science*, vol. 6, no. 21, pp. 25-30, 2020. [Google Scholar] [Publisher Link]

[7]   Bonaventure Onyeka Ekengwu et al., "Effect of PID Tuned Digital Compensator on Servo-Based Ground Station Satellite Antenna Positioning Control System," *In 2nd International Conference on Electrical Power Engineering (ICEPENG)*, pp. 97–101, 2021. [Google Scholar] [Publisher Link]

[8]   Bonaventure Onyeka Ekengwu et al., "Effect of Different Controllers on Performance of Dish Antenna Positioning System for Distributed Mobile Telemedicine Nodes," *Iconic Research and Engineering Journals*, vol. 4, no. 7, pp. 97-103, 2021. [CrossRef] [Publisher Link]

[9]   Sagar Yadav, and Vinni Sharma, "Modelling and Simulation of Elevation Position Control of a Giant Meter Wave Radio Telescope (GMRT) in MATLAB using PID and Controllers," *International Journal of Informative Research in Electrical, Electronics, Instrumentation and Control Engineering*, vol. 4, no. 3, pp. 165–168, 2016. [Google Scholar] [Publisher Link]

[10] Linus A. Alooa, Peter K. Kihatob, and Stanley I. Kamau, "DC Servomotor-Based Antenna Positioning Control System Design using Hybrid PID-LQR Controller," *European International Journal of Science and Technology*, vol. 5, no. 2, pp. 17-31, 2016. [Google Scholar] [Publisher Link]

[11] Abdul Rehman Chishti et al., "Radio Telescope Antenna Azimuth Position Control System Design and Analysis in MATLAB/Simulink using PID & LQR Controller," *Automatic Control and Computer Sciences*, vol. 60, no. 64, pp. 3-4, 2014. [Google Scholar] [Publisher Link]

[12] Aveen Uthman, and Shahdan Sudin, "Antenna Azimuth Position Control System using PID Controller & State-Feedback Controller Approach," *International Journal of Electrical and Computer Engineering*, vol. 8, no. 3, pp. 1539-1550, 2018. [CrossRef] [Google Scholar] [Publisher Link]

[13] E Govinda Kumar et al., "Control of Antenna Azimuth Position using Fractional Order Lead Compensator," *International Journal of Engineering & Technology*, vol. 7, no. 2, pp. 166-171, 2018. [CrossRef] [Google Scholar] [Publisher Link]

[14] Selin Aydın Fandaklı, and Halil İbrahim Okumuş, "Antenna Azimuth Position Control with PID, Fuzzy Logic and Sliding Mode Controllers," *International Symposioum on Innovations in Inteligent Systems and Applications*, pp. 1-5, 2016. [CrossRef] [Google Scholar] [Publisher Link]

[15] Paulinus Chinaenye Eze et al., "Improving the Performance Response of Mobile Satellite Dish Antenna Network within Nigeria," *Journal of Electrical Engineering, Electronics, Control and Computer Science,* vol. 6, no. 21, pp. 25-30, 2020. [Google Scholar] [Publisher Link]

[16] Udai Singh, and Nidhi Singh Pal, "Antenna Azimuth Position Control using Model Reference Adaptive and Self Tuning Controller," *In Proceedings of the International Conference on Advances in Electronics, Electrical & Computational Intelligence (ICAEEC)*, 2019. [Google Scholar] [Publisher Link]

[17] Ahmed Tijani Salawudeen et al., "Optimal Design of PID Controller for Deep Space Antenna Positioning using Weighted Cultural Artificial Fish Swarm Algorithm," *Journal of Electrical & Electronic Systems*, vol. 6, no. 4, 2017. [CrossRef] [Google Scholar] [Publisher Link]

[18] Qilin Zeng, Jiaxin Liu, and Weiming Xiong, "Research on Antennas Alignment of Dynamic Point-to-Point Communication," *Mathematical Problems in Engineering*, vol. 2, pp. 1-5, 2018. [CrossRef] [Google Scholar] [Publisher Link]

[19] Tilak Sarmah, Pranjal Borah, and Tulshi Bezboruah, "Tuning of Microstrip Patch Antenna by Adding an Extra Portion at the Upper End of the Antenna," *International Journal of Engineering Trends and Technology*, vol. 71, no. 4, pp. 474-482, 2023. [CrossRef] [Google Scholar] [Publisher Link]

[20] Benjamin C. Agwah, and Paulinus C. Eze, "An Intelligent Controller Augmented with Variable Zero Lag Compensation for the Antilock Braking System," *International Journal of Mechanical and Mechatronics Engineering*, vol. 16, no. 11, pp. 303-310, 2022. [Google Scholar] [Publisher Link]

[21] Rakesh Goswami, and Dheeraj Joshi, "Performance Review of Fuzzy Logic Based Controllers Employed in Brushless DC Motor," *Procedia Computer Science*, vol. 132, pp. 623-631, 2018. [CrossRef] [Google Scholar] [Publisher Link]

[22] Linus A. Alwal, Peter K. Kihato, and Stanley I. Kamau, "Design of Neuro-Fuzzy System Controller for DC Servomotor-Based Satellite Tracking System," *IOSR Journal of Electrical and Electronics Engineering (IOSR-JEEE)*, vol. 11, no. 4, pp. 89-102, 2016. [CrossRef] [Google Scholar] [Publisher Link]

[23] Ekengwu Bonaventure Onyeka, Muoghalu Chidiebere, and Achebe Patience Nkiruka, "Performance Improvement of Antenna Positioning Control System using Model Predictive Controller," *European Journal of Advances in Engineering and Technology*, vol. 5, no. 9, pp. 722-729, 2018. [Google Scholar] [Publisher Link]

[24] Surbhi Gupta, "Improving Performance and Loss Minimization of Distribution System with 33 Bus Dg System," *International Journal of Engineering Trends and Technology*, vol. 69, no. 1, pp. 132-138, 2021. [CrossRef] [Publisher Link]

[25] Christian Mbaocha, Paulinus Eze, and Valentine Uchegbu, "Positioning Control of Drilling Tool Device for High-Speed Performance," *International Journal of Electrical and Electronics Research*, vol. 3, no. 2, pp. 138-145, 2015. [Google Scholar] [Publisher Link]

[26] Pillalamarri Ravi Kumar, and V. Naga Babu, "Position Control of Servo System using PID Controller Tuning with Soft Computing Optimization Techniques," *International Journal of Engineering Research & Technology*, vol. 3, no. 11, pp. 976-980, 2014. [CrossRef] [Google Scholar] [Publisher Link]

[27] Rucha P. Khadatkar, and D. B. Waghmare, "Damping Power System Oscillations with Controller using STATCOM," *International Journal of Recent Engineering Science*, vol. 5, no. 1, pp. 1-7, 2018. [CrossRef] [Google Scholar] [Publisher Link]

[28] C. N. Moughalu, and P. N. Achebe, "Two-Phase Hybrid Stepping Motor Based Antenna Positioning Control System using Proportional Integral and Derivative Controller," *Iconic Research and Engineering Journals*, vol. 4, no. 10, pp. 152-167, 2021. [Google Scholar] [Publisher Link]

[29] Ugochukwu P. Okoye, P. C. Eze, and Dennis C. Oyiogu, "Enhancing the Performance of AVR System with Prefilter Aided PID Controller," *Access International Journal of Research and Development*, vol. 1, no. 1, pp. 19-32, 2021. [Google Scholar] [Publisher Link]